AN APPROACH FOR THE INCLUSION OF LOADING CONDITIONS IN A POLYHEDRAL-BASED METHOD FOR EARLY VARIATION MANAGEMENT

Restrepo Garcia, Carlos Andres (1,2);
Teissandier, Denis (1);
Anwer, Nabil (2);
Ledoux, Yann (1);
Delos, Vincent (1);
Pierre, Laurent (2);
Garcia Gomez, Sonia Carolina (1)

1: University of Bordeaux;
2: Paris-Saclay University

ABSTRACT

The variation management and product quality processes are important tasks to guarantee the assemblability of the systems, the scrap reduction and to avoid delays on production and launching. The compound of activities in Geometric Dimensioning and Tolerancing (GD&T) are necessary, especially in the early design stages, to take into account variations of different nature and from different sources. In this paper, an approach for considering the loading conditions in a polyhedral-based approach in tolerancing design is presented. The load boundary conditions are represented as additional displacement restrictions in the deviation space. The restrictions imposed by the physical limits of a system, the ones coming from the loading conditions and the degrees of freedom (DoF) can be all described and represented with a single polyhedron operand. The approach is illustrated using a simplified 2-D model for both ideal and non-ideal geometry. A 3-D model describing an unilateral contact is presented as a case study using Skin Model Shapes. By taking into account geometrical form defects, external loads, and the kinematics of the system, its sensitivity to variations can be reduced even from early design stages.

Keywords: Tolerance representation and management, Robust design, Design for X (DfX)

Contact:
Restrepo Garcia, Carlos Andres
University of Bordeaux
France
carlos.restrepo@u-bordeaux.fr

Cite this article: Restrepo Garcia, C. A., Teissandier, D., Anwer, N., Ledoux, Y., Delos, V., Pierre, L., Garcia Gomez, S. C. (2023) 'An Approach for the Inclusion of Loading Conditions in a Polyhedral-Based Method for Early Variation Management', in *Proceedings of the International Conference on Engineering Design (ICED23),* Bordeaux, France, 24-28 July 2023. DOI:10.1017/pds.2023.52

https://doi.org/10.1017/pds.2023.52 Published online by Cambridge University Press

1 INTRODUCTION

The different techniques, methods, metrics and models used to make the development of a product insensitive to variations are grouped under the name of Robust Design Methodology (RDM). There exist many different methods for each one of the stages in the product development process, some of them are more focused on the failure prevention, hence they are more related to reliability than robustness (Bertsche, 2008a,b). Other methods and techniques deal with the reduction of variation in the product development and can be categorized as suggested in (Eifler et al., 2013).

The geometric and dimensional tolerancing activities are indispensable in the uncertainty management and quality control process. From early design stages, the stack-up of variations of the constituting parts of an assembly and the additional deviations induced during the assembly process need to be taken into account. The way of accumulating these variations depends on the representation model chosen. Geometric tolerancing models like the matrix model or the small displacement torsor compute the stack-up of deviations for iso-constraint systems whose joints make a linear or network stack-up type by chaining the different matrices of the functional elements of the assembly together (Polini, 2011). The representation models based on set of constraints, known as well as *Degrees of Freedom* (DoF) or spatials math models, like TTRS, Deviation Domains (Giordano et al., 2007), Tolerance-Maps (Davidson et al., 2002), Polytopes (Arroyave-Tobón et al., 2017) and Polyhedra (Delos et al., 2021) are capable of modeling 3D stack-up deviations in a comprehensive manner, and in the case of the last two, deal with over-constraints mechanisms.

The mobility and restriction of the intended system must be respected with the less possible ambiguity. The kinematic compliance of the system is affected by the individual interfaces involved in the functionality of the same. In (Ebro et al., 2012), the redundant kinematic restrictions (over-constraint contacts) are clarified following a series of design principles from the preliminary design, reducing the ambiguity in design parameters.

The main contribution of this work is to show how the load boundary conditions in rigid assemblies can be represented as additional displacement restrictions in a polyhedral-based approach in tolerancing design. In this way, the geometrical restrictions are derived in three parts using a polyhedron: the purely geometrical restrictions imposed by the physical limits of the contact, or the specification of a surface in a zone; the restrictions coming from the load boundary conditions; and the mobilities of the contact. The Skin Model Shapes presented in this work were generated using the tool explained in (Restrepo Garcia et al., 2022), and it has more information about the generation process of the SMS. The algorithms created used in this model will be incorporated in the same platform and they will allow the contact simulation and stability analysis of a system. The paper is arranged as follows: In section 2 are described the fundamental methods and concepts that will be used in the proposed approach; in section 3 the proposed approach is explained along with some basic examples to illustrate the procedure; in section 4 an unilateral contact case study is presented to further validate the method and in Section 5 advantages, shortcomings and future work are discussed.

2 ASSEMBLY SIMULATION

2.1 Types of contact

The attributes of a contact vary depending on the types of features in contact (plane, cylinder, etc.) and on the type of configuration that binds them. Fig. 1 represents the three cases of an unilateral contact of two planar features. Fig. 1a. shows the case of a floating contact. In a floating contact, the tangential and normal displacements are allowed, meaning that it has all the possible degrees of freedom (DoF) of a mechanical joint. There are works that study this contact configuration in over constraint systems using the virtual work principle or regularized closure functions G (Cammarata, 2017; Rameau et al., 2018). A fixed contact is represented in Fig. 1c., in which all relative movements between the two mating surfaces are restricted, meaning that the contact has zero DoF.

Fig. 1b. represents an unilateral sliding contact. In this case, the tangential displacements are allowed but normal displacements are restricted. The restriction of movement in the direction of the contact surface normal presupposes that a mechanical action (i.e., a force) maintains the two surfaces in contact. In (Liu et al., 2018) the authors represent a bilateral contact pair with form defects using polytopes. In (Yan and Ballu, 2018) Yan and Ballu explore different types of assemblies using Skin Model Shapes

https://doi.org/10.1017/pds.2023.52 Published online by Cambridge University Press

(SMS) and they express the assembly load boundary conditions as additional linear constraints using the *Small Displacement Torsor (SDT)*. The present work focuses on the description and representation of the matting forces in rigid assemblies considering form defects in variation analysis using polyhedra.

2.2 Contact constraints

A 3-dimensional rigid body has six degrees of freedom that can be specified by means of the location and rotation of a local coordinate frame **C** relative to an inertial frame O fixed at the global origin as seen in Fig. 2. The spatial velocity of a part 1 can be expressed in terms of what they call a *twist* (**t**) in screw theory (Siciliano and Khatib, 2016),

$$\mathbf{t} = (\omega^T, v^T), \tag{1}$$

where $\boldsymbol{\omega} = (\omega_x, \omega_y, \omega_z)^T$ is the angular velocity and $\mathbf{v} = (v_x, v_y, v_z)^T$ the linear velocity of point **C** relative to the global frame O, and $\boldsymbol{\omega}$ must satisfy:

$$\dot{\mathbf{r}}_{C/O} = \boldsymbol{\omega} \times \mathbf{r}_{C/O} \tag{2}$$

where $\dot{\mathbf{r}}_{C/O}$ is time derivative of the rotation matrix and $\mathbf{r}_{C/O}$ is the rotation matrix of the part relative to O, and $\mathbf{v}$ must satisfy:

$$\mathbf{v}_C = \dot{\overrightarrow{\mathbf{OC}}} - \boldsymbol{\omega} \times \overrightarrow{\mathbf{OC}} \tag{3}$$

where $\overrightarrow{\mathbf{OC}}$ and $\dot{\overrightarrow{\mathbf{OC}}}$ are the position of the center of mass of the part and its time derivative. Equations 1 to 3 define the spatial velocity of part 1 which is composed of the angular velocity of the part expressed in the global frame and the linear velocity of a point rigidly attached to the part but as if it were already at the global origin.

We can describe the linear velocity of a contact point P_c which provides an unilateral restriction that restraints its movement towards the part 2 as:

$$\mathbf{v}_{P_c} = \mathbf{v}_C + \boldsymbol{\omega} \times \overrightarrow{\mathbf{OP}}_c \tag{4}$$

The non-interpenetration condition for the unilateral restriction can be written as:

$$\mathbf{v}_{P_c} \cdot \hat{\mathbf{u}} = (\mathbf{v}_C + \boldsymbol{\omega} \times \overrightarrow{\mathbf{OP}}_c) \cdot \hat{\mathbf{u}} \geq 0 \tag{5}$$

In Eq. 5, $\hat{u}$ is the contact point normal in the direction of the part 1. This equation expresses the impossibility of the existence of a component of the velocity at the point of contact (P_c) in the opposite direction of the contact normal. For the unilateral contact to be maintained there must exist a force that binds the two parts together. This force acts at P_c in the contact normal direction $\hat{u}$, and it generates a moment around O. A force acting on a rigid body defines a *wrench*, as it can be seen in Eq. 6. For a unit force, Eq. 6 can be written as shown in Eq. 7.

$$\mathbf{w} = (\mathbf{m}^T, \mathbf{f}^T)^T \tag{6}$$

$$\mathbf{w} = [(\overrightarrow{\mathbf{OP}}_c \times \hat{\mathbf{u}})^T, \hat{\mathbf{u}}^T]^T \tag{7}$$

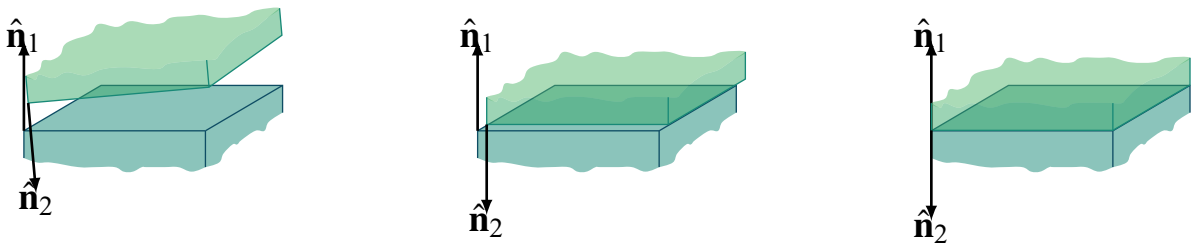

(a) Floating contact (b) Sliding contact (c) Fixed contact

Figure 1. Cases of contact of two plane features

https://doi.org/10.1017/pds.2023.52 Published online by Cambridge University Press

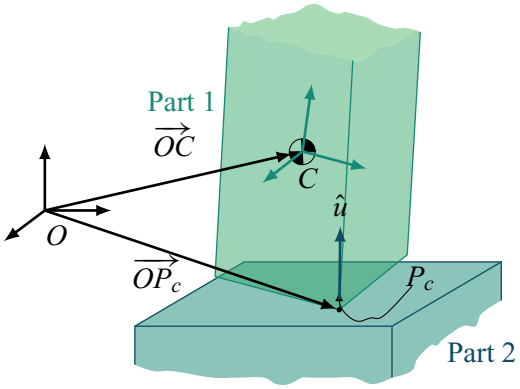

Figure 2. Kinematics of a contact in rigid body models

The non-interpenetration condition for unilateral restriction in Eq. 5 can be expressed in terms of the *twist* and *wrench* as shown in Eq. 8 if the constraint is stationary.

$$\mathbf{t}^T\mathbf{w} \geq 0 \tag{8}$$

Each of the inequalities in Eq. 8 generates a half-space that constraints the six-dimensional velocity domain. The intersection of a finite number of restrictions describes a convex polyhedron that represents the feasible part velocities, and for the stationary case, all the half-spaces pass through the origin of the velocity domain.

The approach that will be detailed in Section 3 is based on the contact constraints generally used in kinematics of robots. The formalization of the force as an additional restriction in the deviation domain is presented for unilateral contacts in rigid-body models.

2.3 Polyhedra approach in tolerance analysis

The approach based on polyhedra in tolerance analysis consists in representing the dimensional, geometric or contact restrictions imposed by design specifications as a set of constraints in the form of inequalities. For bilateral contacts, the intersection of a set of half-spaces defines a polytope P that constitutes the bounded part of a polyhedron as shown in Eq. 9

$$\Gamma = P \oplus C \tag{9}$$

A polyhedron can be decomposed as the sum of a polytope P, result of the intersection of a finite number of halfspaces ($P = \cap_i \bar{H}_i^+$), and a polyhedral cone $C = \sum \Delta k$ (a sum of straight lines) that relates to the degrees of invariance of a toleranced feature or to the degrees of freedom of a joint Delos et al. (2021). The analysis of any kinematic pair resulting from the matting of any two type of surfaces can be modeled by means of polyhedra: manipulating polytopes for the restricted displacements, and a set of straight lines for the allowable displacements.

For the types of contact in Fig. 1, the polyhedron for the *floating* contact case is constituted of an affine space of dimension d for the straight lines and its associated polytope is of dimension $(6 - d)$, where d is the degrees of freedom; for the *sliding* contact case, the straight lines describe an affine space of dimension d, but its associated polytope is a singleton of dimension $(6 - d)$; for a *fixed* contact, the straight lines describe a singleton of dimension d and its polytope is a singleton of dimension $(6 - d)$.

3 MATTING FORCES AS HALF-SPACES

The work presented here is aligned with the method presented in Sec. 2.2 and since we are dealing with rigid body displacements, the Small Displacement Torsor (SDT) theory is subjacent when describing the displacements of a surface as described in Alex Ballu, Jean-Yves Dantan (2010). To illustrate the method proposed in this work, it is necessary to review the basic assumptions underlying the definition of a unilateral contact using polyhedra.

Two plane surfaces S_1 and S_2 with no form deviations define an unilateral contact represented in 2D in Fig. 3. The contact element is defined from the intersection of both surfaces and it is discretized in four points (P_1 to P_4). The contact restrictions are written in the middle at point M. By fixing the clearance

https://doi.org/10.1017/pds.2023.52 Published online by Cambridge University Press

between the two surfaces to 0, the equation that describes the contact restrictions on each one of the discretization nodes on the contact element and that gives as a result a set of halfspaces, can be written as shown in Eq. 10.

$$\bar{H}_i^+ : (\overrightarrow{t_M} + \overrightarrow{P_iM} \times \overrightarrow{r}) \cdot \hat{n}_i \geq 0 \tag{10}$$

The term $\overrightarrow{t_M}$ is the translation vector of point M ($\overrightarrow{t}_M[t_{Mx}, t_{My}, t_{Mz}]$), $\overrightarrow{P_iM}$ is the position vector of the discretization node P_i in relation to the calculation point M, $\overrightarrow{r}$ ($[r_x, r_y, r_z]$) is the rotation vector of the contact element and $\hat{n}_i$ is node normal, assumed in the y direction for this case.

Each one of the inequalities that arises from Eq. 10 describes a half-space that constraints the subspace of bounded displacements, here translations along y (t_y) and rotations around z (r_z). The superscript $+$ in $\bar{H}_i^+$ means that we remain with the positive part of the half-space and the bar at the top means that the boundary of the half-space is included, so $\bar{H}_1^+$ represents the restriction coming from the node P_1, $\bar{H}_2^+$ from node P_2, etc. The intersection of the set of restrictions written at point M gives as a result the convex polyhedron depicted as the darker region in between half-spaces $\bar{H}_1^+$ and $\bar{H}_4^+$ in Fig. 3a. A restriction can create redundant half-spaces as in the case of the restrictions coming from nodes P_2 and P_3, meaning that the nodes at both extremities of the contact element (P_1 and P_4) are the ones imposing the more restrictive conditions on the contact. In this case, due to the unilateralism of the contact and to its zero clearance all the restrictions pass through the origin of the subspace of bounded displacements and they describe an open operand.

In the unilateral nature of the contact underlies the assumption that there is a force that maintains the contact in place. The neglect in the inclusion of a formalism to explicitly describe the action of a force in unilateral contacts is not significantly important when dealing with ideal features, but it will become important when dealing with skin model shapes as it will be shown later in this section.

The action of an external force $\overrightarrow{\mathbf{F}}$ binds the surfaces together preventing partially or fully the relative displacements between them, and translates into an additional half-space in this method. For the consideration of the action of the force in the polyhedra method is necessary to:

- verify that the restriction induced by the force(s) is/are included in the subspace of bounded displacements; and
- verify that the additional restriction turns the open subspace of bounded displacements into a close one.

In Fig. 3b. the depicted force acts on S_1 pushing it against S_2 at the level of node P_2. The resultant force and torque can be expressed as shown in Eq. 11. The magnitude of the force in this case is not important as we are dealing with rigid bodies, so it can be taken as a unit force along a direction. The action of the force and torque can be translated into a half-space in 6-dimensional space of deviations as shown in Eq. 12, where (x_1, x_2, x_3) correspond to the rotation variables (torques), and (x_4, x_5, x_6) to the translation

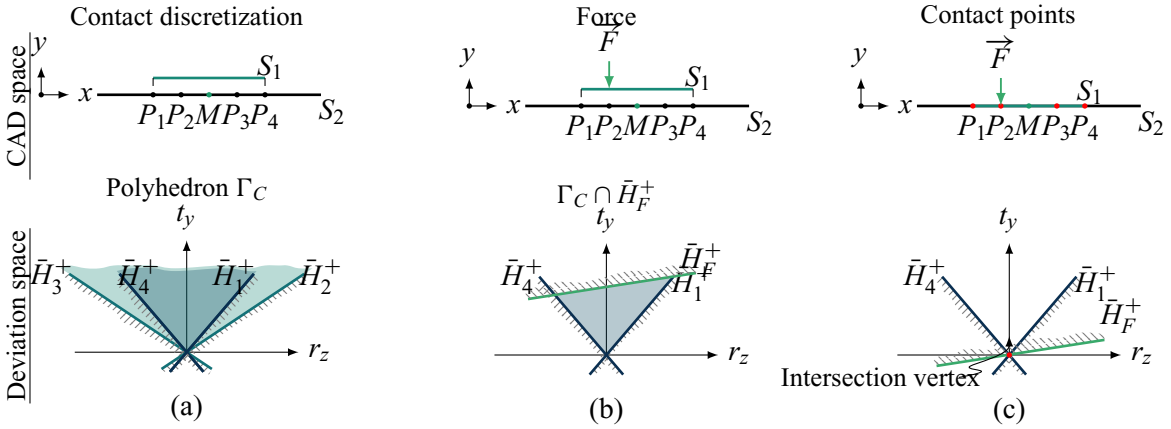

Figure 3. Unilateral contact with no form defects

https://doi.org/10.1017/pds.2023.52 Published online by Cambridge University Press

variables (forces).

$$\begin{cases} \sum F \cdot \hat{n} \\ \sum \overrightarrow{PM} \times (F \cdot \hat{n}) \end{cases} \tag{11}$$

The additional restriction coming from the loads is described in the same way as the half-spaces coming from the contact restrictions, its only difference resides on the value of b_k, referred here as *second member*, which does not take a fixed value, but rather any value that closes the operand. It could be seen as a floating half-space in the subspace of bounded displacements that bounds the operand.

$$\bar{H}_F^+ = \{\mathbf{x} \in \mathbb{R}^6 : b_k + a_{k1}x_1 + ... + a_{k6}x_6 \geq 0\} \tag{12}$$

The verification of the first condition, mentioned above in the bullet list, to maintain in position the parts consists in checking the inclusion of the additional restriction in the subspace of bounded displacements, meaning that there should not exist forces acting in the direction of the DoFs, which is a necessary condition for kinematic compliance. It can be written simply as: $\Delta k \perp \vec{F}$. The fulfilment of the second condition, the bounding condition, depends on two aspects related to the load: its point of the application and its orientation. In this manner, what is being said is that the resultant of a system of forces must lie in the physical limits of the contact element, in between P_1 and P_4; and that the forces are applied in the direction that actually binds the two surfaces together, along $-y$ in this case.

Once the conditions are verified, the points where the two features touch each other can be found from the deviation space. To do so, it is necessary to search for the farthest point of the polyhedron in relation to the additional half-space (force), or to find the point (or points) that minimizes the volume of the operand after bounding. That point is generated from the intersection of several half-spaces, which are themselves coming from actual nodes on the contact element in the geometric space. In this way, a point in the subspace of bounded displacements will retrieve the nodes on the actual contact element. In this case, the solution is trivial as shown in Fig. 3c, the farthest point is the one coming from the intersection of all the half-spaces, meaning that all the nodes in one feature are in contact with the nodes in the other. This is always the case for planar features with no form deviations.

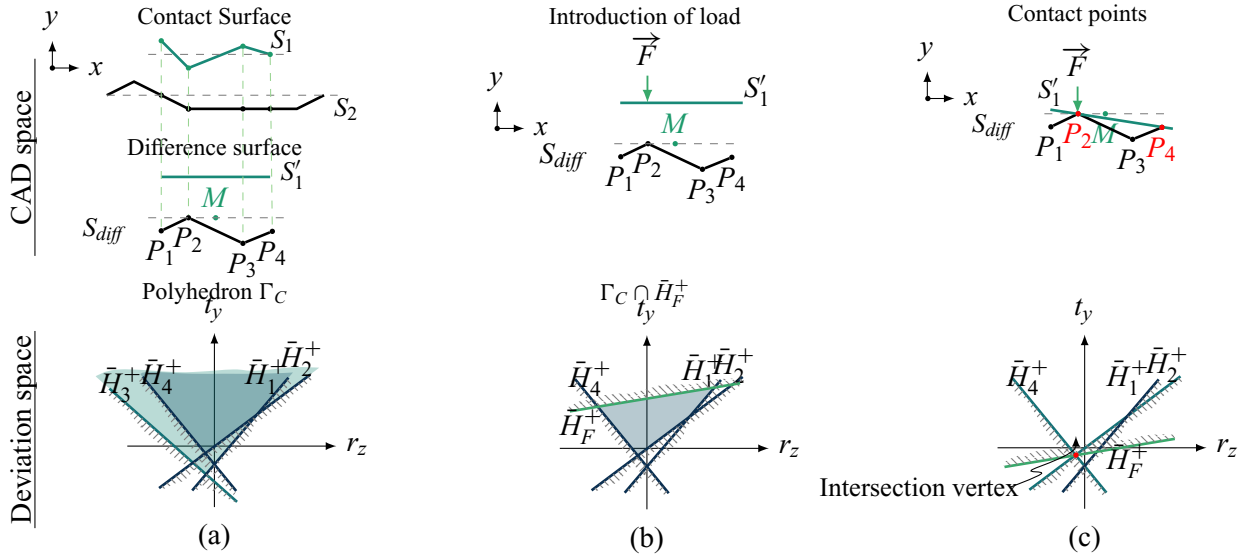

Figure 4. Unilateral contact with form defects

When we are dealing with form defects the described approach does not change, but the topology of the polyhedra operands will impact the result. Two surfaces with defects S_1 and S_2 are presented at the top part of Fig. 4a. One of the methods to establish the contact between features with form defects, proposed in Samper et al. (2009), consists in establishing the contact between a *difference surface* (S_{diff}), which is an equivalent surface that describes the combined effect of the deviations of both features, and a surface of perfect form S_1'. The representation of such surfaces is shown in the middle part of Fig. 4a.

https://doi.org/10.1017/pds.2023.52 Published online by Cambridge University Press

The operand produced by the unilateral contact restrictions of the difference surface with a perfect planar feature is presented at the bottom part of Fig. 4a. As it can be seen, the topology of the operand changes; the restrictions coming from the discretization nodes produce more non-redundant half-spaces, and their intersection is no longer the origin of the deviation space.
If the load is applied at the same point than before, pushing the perfect planar feature against the difference surface, the additional restriction could close the operand as depicted in Fig. 4b. It is easily inferable that the result of the search for the farthest point will change according to the orientation of the additional half-space in the subspace of bounded displacements. In this case, the orientation of the half-space produced by the force depends on its point of application, thus if the load were applied at the same node where the contact restrictions were written, the half-space would be perpendicular to the axis of translation along y (t_y).
As shown in Fig. 4c. the farthest point comes from the intersection of half-spaces $\bar{H}_2^+$ and $\bar{H}_4^+$ which are generated by points P_2 and P_4 that are the two points of the difference surface that are in contact with the planar feature.
In the next section, an example of a simple assembly is presented to illustrate the advantages of the proposed method.

4 APPLICATION AND ANALYSIS

The example used in this work is a simplified model of gas turbine made up of a ring and a pipe. The ring has three holes and the pipe three pins for the relative positioning of the parts. The two parts are kept in contact by means of three bolts distributed along the pitch circle diameter and spaced 120 degrees between them. The forces ($\vec{F}_1, \vec{F}_2, \vec{F}_3$) shown in Fig. 5a. represent the action of such bolts. The resultant force of the three bolts ($\vec{F}$) is acting in the center of the circle along $-x$. The two surfaces in contact have different mesh densities. The ring mesh has 368 nodes and 736 triangles; the pipe mesh has 454 nodes and 908 triangles. The two surfaces are nominally two perfect planes in the CAD model.

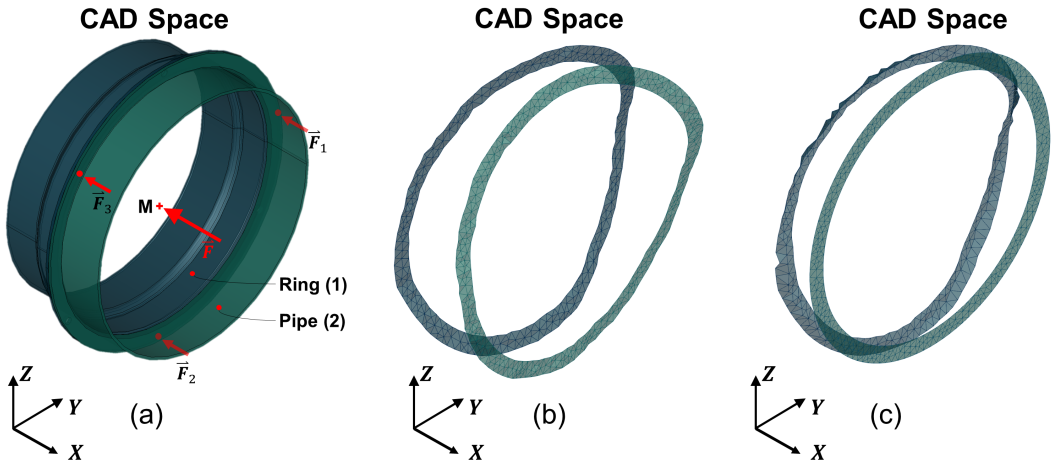

Figure 5. Nominal model, skin model shapes and surface of difference

Table 1 describes the kinematic pairs in the assembly. $S_{1,1}$ and $S_{2,1}$ refer to the planar contact between the ring (1) and the pipe (2); Features $S_{1,2}$ to $S_{1,4}$, and $S_{2,2}$ to $S_{2,4}$ refer to the contact surfaces between the three holes in the ring and the three pins in the pipe. There are no degrees of freedom in the final assembly: the mobilities allowed by the planar contact are restraint by the pin-hole contacts. In the next part of this section, only the planar contact is studied, its degrees of freedom are modelled as a set of straight lines Δk, the restrictions imposed by the contact describe a polyhedron in a subspace orthogonal to the subspace of the mobilities as shown in Eq. 9. The loading conditions were incorporated to the approach as an additional half-space in the subspace of bounded displacements, thereby we can describe the kinematic behaviour of the contact and take into account the loading conditions with a single polyhedral operand.

https://doi.org/10.1017/pds.2023.52 Published online by Cambridge University Press

Table 1. Kinematics of contacts elements

Features in contact	*Type of contact*	*Degrees of freedom*					
		$\mathbf{t}_x$	$\mathbf{t}_y$	$\mathbf{t}_z$	$\mathbf{r}_x$	$\mathbf{r}_y$	$\mathbf{r}_z$
$S_{1,1}$, $S_{2,1}$	Planar pair	0	1	1	1	0	0
$S_{1,2}$, $S_{2,2}$	Ball-and-cylindrical	1	0	0	1	1	1
$S_{1,3}$, $S_{2,3}$	Ball-and-cylindrical	1	0	0	1	1	1
$S_{1,4}$, $S_{2,4}$	Ball-and-cylindrical	1	0	0	1	1	1
0 =*Suppressed*, 1 =*Free*							

4.1 Deviation modelling - skin model shapes

The deviation modelling was carried out using PolitoCAT (Restrepo Garcia et al., 2022), both systematic and random deviations were used for each of the features. For systematic deviations, a modal approach based on vibration modes was used. For random deviations, the Gaussian random fields method was used. The discrete representation of the Skin Model Shapes (SMS) is shown in Fig. 5b.

The difference surface method was used to establish the contact between the features with form defects. As it was previously mentioned, this method consists in calculating an equivalent surface that embodies the deviations of two features in contact transforming the contact of two features with form defects into the contact of an equivalent feature and a feature with no deviations. The representation of such a surface is shown in Fig. 5c.

The loading conditions shown in Fig. 5a. are simply transposed to the surfaces in contact as shown in Fig. 6a. The two planar surfaces are allowed to move relatively to each other in translation along **y** and **z**, and in rotation along **x**. The subspace of bounded displacements is then constituted of the rotations along **y** and **z** (r_y, r_z), and the translation along **x** ($\mathbf{t}_x$) that will be restricted by the external force.

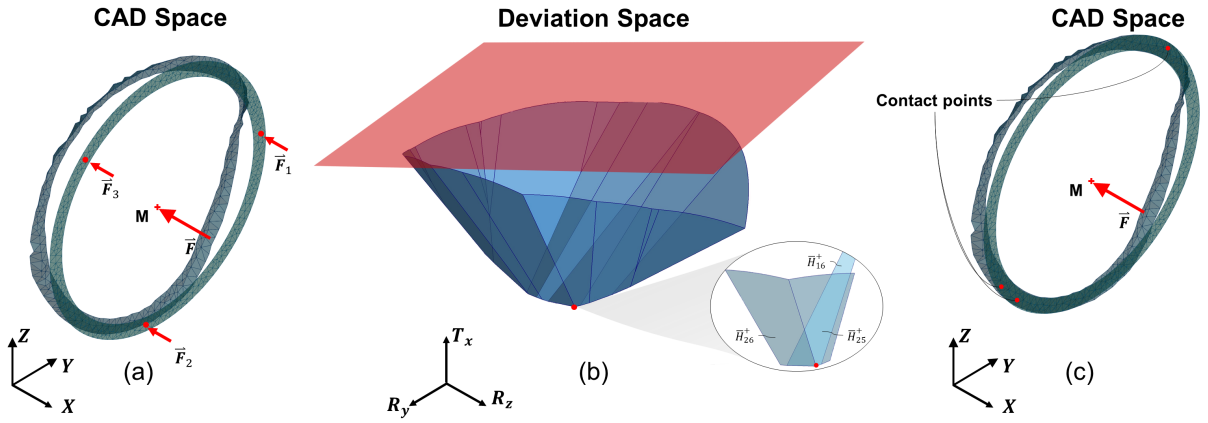

Figure 6. Difference surface, polyhedron with additional half-space and contact points

Calculating the polyhedron operand of the SMS will necessarily complexify the topology of the resulting polyhedron, but not as much as one might think. Actually, for the deviations showed in Fig. 5c. only 21 half-spaces are relevant for constructing the polyhedron, the restrictions coming from the all the other points are simply redundant in this case. The complexity of the resulting operand depends on the type of contact being modeled and the instance of skin model shape itself.

The resulting polyhedron of the contact with form defects is presented in Fig. 6b. All the restrictions were written at point **M** whose coordinates are $(0,0,0)$. The additional restriction is depicted as the red half-space on top of the operand. It comes from the resultant action of the three bolts at point M.

As explained above, the search for the farthest point will give as result, in stable cases, a point in the subspace of bounded displacements that comes from the intersection of at least as many half-spaces as the dimension of the same subspace. Since there is a complete traceability from the vertices in the

https://doi.org/10.1017/pds.2023.52 Published online by Cambridge University Press

polyhedron to the actual nodes were the contact restrictions were written, we can know which points are in contact given a specific load case. Here, the points in contact are shown in Fig. 6c. The red dots show the nodes on the difference surface that are in contact with the nominal planar feature of the pipe.

5 DISCUSSION AND CONCLUSIONS

The inevitable variations during the product and process development can be taken into account from early design stages; tolerance analysis, the inclusion of new paradigms like the SMS, and the incorporation of loads in the assembly process are ways to consider beforehand some the variations that will cause systematic deviations on the parts, reduction on the quality of the pieces, scraps and delays on production and launching of products.

In this work, a method that exploits the advantages of the deviation space and duality properties of the screw theory was presented for determining the contact between matting features with form defects in rigid-body models. This method enables the explicit description of not only displacement restrictions but also restrictions imposed by loading. The presented method has the advantage that can be generalized for any type of contact since the determination of the nodes in contact in the geometry is carried out in the deviation space and not in the geometric one. It is also the starting point for a stability analysis of the system; if for instance, the additional half-space happens to be at the same maximum distance from several vertices, it would mean that additional half-space is parallel to a line or facet of the contact polyhedron. We would obtain as a result more nodes than needed in the geometry, allowing us to track unstable zones in the geometry. The study of instability exploiting the advantages of the deviation space is one of our outgoing research topics.

REFERENCES

Alex Ballu, Jean-Yves Dantan, L.M. (2010), "Geometric Tolerancing Languages Language of Tolerancing : GeoSpelling", in: L.M. Francois Villeneuve (Editor), *Geometric Tolerancing of Products*, chapter Chapter 2, ISTE Ltd, pp. 23–53.

Arroyave-Tobón, S., Teissandier, D. and Delos, V. (2017), "Tolerance Analysis with Polytopes in HV-Description", *Journal of Computing and Information Science in Engineering*, Vol. 17 No. 4, pp. 1–9, http://doi.org/10.1115/1.4036558.

Bertsche, B. (2008a), "Reliability in Automotive and Mechanical Engineering", in: *Reliability in Automotive and Mechanical Engineering*, chapter 4 FMEA F, Springer-Verlag Berlin Heidelberg, pp. 98–159, http://doi.org/10.1007/978-3-540-34282-3.

Bertsche, B. (2008b), "Reliability in Automotive and Mechanical Engineering", in: *Reliability in Automotive and Mechanical Engineering*, chapter 5 FTA, Springer-Verlag Berlin Heidelberg, pp. 160–190, http://doi.org/10.1007/978-3-540-34282-3.

Cammarata, A. (2017), "A novel method to determine position and orientation errors in clearance-affected over-constrained mechanisms", *Mechanism and Machine Theory*, Vol. 118, pp. 247–264, http://doi.org/10.1016/2017.08.012.

Davidson, J.K., Mujezinović, A. and Shah, J.J. (2002), "A new mathematical model for geometric tolerances as applied to round faces", *Journal of Mechanical Design, Transactions of the ASME*, Vol. 124 No. 4, pp. 609–622, http://doi.org/10.1115/1.1497362.

Delos, V., Teissandier, D., Malyshev, A., Nuel, G. and García, S.C. (2021), "Polyhedral-based Modeling and Algorithms for Tolerancing Analysis", *CAD Computer Aided Design*, Vol. 141, p. 103071, http://doi.org/10.1016/j.cad.2021.103071.

Ebro, M., Howard, T.J. and Rasmussen, J.J. (2012), "The foundation for robust design: Enabling robustness through kinematic design and design clarity", *Proceedings of International Design Conference, DESIGN*, Vol. DS 70, pp. 817–826.

Eifler, T., Ebro, M. and Howard, T.J. (2013), "A classification of the industrial relevance of robust design methods", *Proceedings of the International Conference on Engineering Design, ICED*, Vol. 9 DS75-09 No. August, pp. 427–436.

Giordano, M., Samper, S. and Petit, J.P. (2007), "Tolerance analysis and synthesis by means of deviation domains, axi-symmetric cases", in: J.K. Davidson (Editor), *Models for Computer Aided Tolerancing in Design and Manufacturing*, Springer Netherlands, Dordrecht, pp. 85–94.

Liu, J., Zhang, Z., Ding, X. and Shao, N. (2018), "Integrating form errors and local surface deformations into tolerance analysis based on skin model shapes and a boundary element method", *CAD Computer Aided Design*, Vol. 104, pp. 45–59, http://doi.org/10.1016/j.cad.2018.05.005.

https://doi.org/10.1017/pds.2023.52 Published online by Cambridge University Press

Polini, W. (2011), "Geometric Tolerance Analysis", in: B.M. Colosimo and N. Senin (Editors), *Geometric Tolerances: Impact on Product Design, Quality Inspection and Statistical Process Monitoring*, Springer London, pp. 39–68, http://doi.org/10.1007/978-1-84996-311-4-2.

Rameau, J.F., Serré, P. and Moinet, M. (2018), "Clearance vs. tolerance for rigid overconstrained assemblies", *CAD Computer Aided Design*, Vol. 97, pp. 27–40, http://doi.org/10.1016/j.cad.2017.12.001.

Restrepo Garcia, C.A., Teissandier, D., Anwer, N., Delos, V., Ledoux, Y. and Pierre, L. (2022), "An integrated open source CAT based on Skin Model Shapes", in: *17th CIRP Conference on Computer Aided Tolerancing*, Vol. 114, Elsevier B.V., pp. 1–6, http://doi.org/10.1016/j.procir.2022.10.020. https://hal.archives-ouvertes.fr/hal-03696571/

Samper, S., Adragna, P.A., Favreliere, H. and Pillet, M. (2009), "Modeling of 2D and 3D assemblies taking into account form errors of plane surfaces", *Journal of Computing and Information Science in Engineering*, Vol. 9 No. 4, pp. 1–12, http://doi.org/10.1115/1.3249575.

Siciliano, B. and Khatib, O. (2016), *Springer handbook of robotics*, Springer Berlin Heidelberg, http://doi.org/10.1007/978-3-319-32552-1.

Yan, X. and Ballu, A. (2018), "Tolerance analysis using skin model shapes and linear complementarity conditions", *Journal of Manufacturing Systems*, Vol. 48 No. July, pp. 140–156, http://doi.org/10.1016/j.jmsy.2018.07.005.

https://doi.org/10.1017/pds.2023.52 Published online by Cambridge University Press